

[Click here to view linked References](#)

Authors:

Inari Avila*, Konstantin Pantchev*, Jani Holopainen**, Mikko Ritala**, Juha Tuukkanen*

Adhesion and mechanical properties of nanocrystalline hydroxyapatite coating obtained by conversion of atomic layer deposited calcium carbonate on titanium substrate

Affiliations and addresses of the authors:

*Department of Anatomy and Cell Biology, Institute of Cancer Research and Translational Medicine, Medical Research Center, University of Oulu, Oulu, Finland

**Department of Chemistry, University of Helsinki, P.O. Box 55, FI-00014 Helsinki, Finland

Corresponding author:

Inari Avila, Inari.avila@oulu.fi, +358 050 4877 434, ORCID iD 0000-0002-8310-1741

ABSTRACT

The purpose of this study was to evaluate the mechanical properties of nanocrystalline hydroxyapatite coating by tensile adhesion testing and scratch testing. The coating was manufactured on titanium substrate by converting atomic layer deposited (ALD) calcium carbonate thin film in dilute phosphate solution. The tensile adhesion testing was performed with hydraulic testing device in accordance with ISO 4624 and ISO 16276-1. Scratch testing was done according to SFS-EN 13523-12 with spherical $\varnothing 10 \mu\text{m}$ scratching tip. Characterization of the samples was done with light and electron microscopy after which they were stained with alizarin red and the failure modes and loadings were analyzed.

The highest obtained tensile adhesion value was 6.71 MPa produced with 4000 ALD cycles, converted to hydroxyapatite in alkaline solution and annealed for 30 min in 700°C. The annealing improved the adhesion values by approximately 0.8 MPa, but examining the samples with electron microscopy showed intact coating in both annealed and non-annealed samples. Samples produced with 4000 cycles performed better in testing than 2000 cycle samples, and better adhesion was also achieved with alkaline conversion solution compared to neutral solution.

Keywords: hydroxyapatite, calcium carbonate, adhesion, atomic layer deposition, titanium

1. INTRODUCTION

The number of joint replacement surgeries has increased over the last few decades along with aging population and prolonged life expectancy. This has created a need for developing current implant technologies to improve osseointegration and implant long-term survival rates, thus decreasing the amount of revision surgeries and complications. Titanium and its alloys are widely used in biomedical applications because of their good mechanical properties, such as strength and durability, resistance to corrosion and biocompatibility [1]. Titanium however does not promote apatite formation and thus its bone-bonding abilities are less than ideal in physiological environment, and in order to improve the adhesion a wide range of surface modifications have been utilized over the years[1-3].

In addition to mechanical surface modifications a number of biologically active coating materials have been studied to improve the bioactivity of titanium, including bioactive ceramics such as bioglass [4] and hydroxyapatite ($\text{Ca}_{10}(\text{PO}_4)_6(\text{OH})_2$, HA) [5]. The synthetic HA imitates biological calcium-deficient hydroxyapatite found in human body [6], and it has been shown to promote implant integration directly to bone without intermittent connective tissue layer [7-9]. Metallic implants release ions into the surrounding environment which can lead to foreign body reaction and loosening of the implant [10], and it has been suggested that coating with bioactive material can also reduce the metal ion release from implants [11]. The optimal HA coating material should have as high as possible chemical purity ($\geq 95\%$) with Ca/P-ratio close to stoichiometric 1.67 and the microstructure should imitate crystals found in human bone [5, 12]. Coating layer thickness should be controlled, since thick HA layers have typically weaker mechanical properties, and they will smoothen out possible micro-scale modifications made to the substrate surface [5, 13].

Several coating methods have been developed to produce hydroxyapatite coatings on metal implants, e.g. plasma spraying [14, 15], sol-gel technique [16, 17], pulsed laser deposition [15, 18], magnetron sputtering [19] and electrophoretic deposition [20, 21]. Plasma spraying of titanium implants has been studied intensively over the years and there is evidence *in vivo* [9] and from clinical use [7] of its strong osteoconductive properties. Plasma spraying is

1
2
3
4 suitable for producing cost-effectively coatings with thickness between 30 to 200 μm [2], but
5
6 plasma sprayed coatings suffer from low cohesive strength [22] and high process temperatures
7
8 that can cause inhomogeneity of the chemical composition and/or crystal structure [23, 24],
9
10 and induce cracking of the HA layer. To improve the coating adhesion and crystalline structure
11
12 there have been studies with post-deposition heat treatments [25], but due to residual stresses
13
14 caused by different thermal expansion coefficients the annealing can cause crack formation
15
16 [26] and delamination of the coating in physiological environment [27]. Plasma spraying is
17
18 also a line-of-sight method [28], which limits its use to simple two-dimensional geometries,
19
20 and thick coating layers easily mask substrate surface features meant to improve coating
21
22 adhesion and cell integration [13].

23
24 Atomic layer deposition (ALD) is a form of chemical vapor deposition technique that is used
25
26 for creating highly conformal thin film layers on various substrate materials [29]. ALD is
27
28 based on self-limiting surface reactions of typically two gaseous precursor chemicals that are
29
30 supplied sequentially into a reaction chamber, and the final coating thickness can be controlled
31
32 on atomic level by adjusting the number of reaction cycles [30]. Calcium or calcium-
33
34 containing thin films, such as calcium oxide (CaO), have been deposited by ALD using
35
36 $\text{Ca}(\text{thd})_2$ (thd=2,2,6,6,-tetramethyl-3,5-heptanedionato) [31] or cyclopentadiene type precursor
37
38 [32] as calcium source. Different precursor compositions have been studied as phosphorous
39
40 source, e.g. PH_3 [33], or $(\text{CH}_3\text{O})_3\text{PO}$ [34]. Putkonen et al. [35] described a method to produce
41
42 calcium phosphate layer by ALD using a combination of $\text{Ca}(\text{thd})_2/\text{O}_3$ - and $(\text{CH}_3\text{O})_3\text{PO}/\text{H}_2\text{O}$ -
43
44 precursors. They succeeded in producing amorphous calcium phosphate thin films in
45
46 relatively low process temperatures, and they were able to adjust the phosphorous to calcium
47
48 ratio by carefully controlling the ALD precursor materials' pulsing ratio. However, a high
49
50 temperature ($>500\text{ }^\circ\text{C}$) post-deposition annealing in moist nitrogen was required to crystallize
51
52 the films to hydroxyapatite.

53
54 Holopainen et al. [13] developed a method for manufacturing very thin, uniform layer of
55
56 nanocrystalline hydroxyapatite from atomic layer deposited calcium carbonate thin film. The
57
58 calcium carbonate layer was deposited on top of titanium substrate by ALD using $\text{Ca}(\text{thd})_2$
59
60 and O_3 as precursor materials and converted into hydroxyapatite by immersing the substrate
61
62
63
64
65

into pre-heated dilute phosphate solution. The benefits of this method are low process temperatures, superior penetration and coverage of complex three-dimensional shapes, small final coating layer thickness and stability in biological environment. In this paper we continue the development of this coating method and compare the mechanical adhesion of several versions of this nanocrystalline HA coating material to define the most suitable option for implant use. The mechanical properties are evaluated using tensile adhesion and scratching test methods, and we also evaluate the failure methods and interfaces after testing using light and electron microscopy.

2. MATERIALS AND METHODS

2.1 Film preparation

Thin films of calcium carbonate (CaCO_3) were deposited in F-120 ALD reactor (ASM Microchemistry Ltd., Finland) under nitrogen atmosphere and approximately 5-10 mbar pressure. High-purity N_2 was used as a carrier and purging gas. Substrate material used for these studies was 50 x 50 x 1 mm³ unpolished Grade 2 Titanium sheet (William Gregor Ltd., London, UK), meeting the ASTM B265 specifications. For cross-section thickness analyses some films were also grown on silicon. Substrates were cleaned in ultrasonic bath, rinsed with ethanol and blown dry with nitrogen gas prior to deposition.

$\text{Ca}(\text{thd})_2\text{-O}_3$ ALD process was used to produce calcium carbonate thin films as previously described by Nilsen et al. [30] Ozone gas was generated by feeding pure O_2 (99.9999%) into a Wedeco Ozomatic Modular 4 HC Lab ozone generator, and $\text{Ca}(\text{thd})_2$ (Volatec Oy, Finland) was evaporated from an open source boat at 188 °C. Process temperature was 250 °C, and samples were produced with 2000 and 4000 ALD cycles, with resulting calcium carbonate thin film thicknesses of 95 nm and 190 nm.

CaCO_3 thin films were converted to nanocrystalline hydroxyapatite by immersing the substrates for 1 min in dilute phosphate solutions preheated to 95 °C. Conversion solutions

were manufactured by dissolving diammonium hydrogen phosphate (DAP, $(\text{NH}_4)_2\text{HPO}_4$, Merck, 99%) into concentration of 0.2 M in deionized water or 1M NH_3 solution. After treatment, the samples were rinsed with deionized water and blown dry with compressed air.

2.2 Characterization

Adhesion of nanocrystalline hydroxyapatite layer on titanium substrate was measured by Positest ATA20 hydraulic adhesion tester (DeFelsko Co., USA) in accordance with ISO 4624 and ISO 16276-1. Test plates (approximate size $25 \times 25 \times 1 \text{ mm}^3$) were cleaned by sonication in 100 % ethanol for 3 min. Self-aligning aluminium dollies with 10 mm diameter were roughened with sandpaper (P80) and cleaned by sonication in 100 % ethanol for 3 min. Dollies were then glued with an epoxy resin adhesive (Loctite EA9466 or EA9497) to a coated titanium plate and were left to cure in room temperature for minimum of 48 hours. Tests were repeated four times for each sample type, and used pull rate was 1.0 MPa/s.

Scrath testing was carried out according to SFS-EN 13523-12. Scratches were produced using a 10 μm spherical diamond tip with a minimum distance between consecutive scratches at least 4 mm to ensure independent behaviour of each scratch. Two sets of scratches were produced with Instron 3366 on test plates: short scratches (5 mm) with constant loads and longer scratches (40 mm) with step-wise increasing loads. Short scratches were produced with table speed of 0.1 mm/s and the loading increased from 0 N with approximately 15 mN steps between parallel scratches to maximum load of 122 mN. With long scratches the loading was increased in 4 mm intervals starting from 0 N up to highest load of 370 mN with table speed of 0.2 mm/s, and a total of six identical scratch traces were produced on each sample. Tested samples were produced with alkaline conversion solution and either 2000 or 4000 ALD process cycles.

Film crystallinity was examined by X-ray diffraction (XRD) with a PANalytical X'Pert Pro MPD diffractometer using $\text{CuK}\alpha$ radiation in grazing incidence geometry and an incident angle of 1° . The hydroxyapatite films as-prepared and after adhesion and scratch testing were characterized with field emission scanning electron microscopy (Hitachi S-4800 and Sigma

HD VP FE-SEM). Some samples were sputter coated with a 4 nm layer of Au/Pd prior to FE-SEM imaging to improve image quality. Film thicknesses were evaluated from FE-SEM cross sections from the edges of unpolished samples cut from of HA films on silicon. Samples were stained after adhesion testing with alizarin red that binds to calcium by preparing 2 % solution of the dye in deionized water, and pH of the solution was adjusted to 5.7 with 1 M NaOH. Samples were immersed in the dye for 10 seconds and the extra dye was rinsed with deionized water and blown dry with compressed air.

2.3 Statistical analysis

All quantitative data are expressed as mean \pm standard deviation. Differences between means were analysed for statistical significance using Student's t-test for independent samples. Statistical significance was considered at $p < 0.05$. All data were analyzed using IBM SPSS Statistics v. 24.0 software.

3. RESULTS

All of the prepared hydroxyapatite films had a plate-like hydroxyapatite crystal structure as identified with FE-SEM and XRD (Fig. 1). No significant differences were observed in the surface morphology between the films converted from 2000 and 4000 cycle CaCO_3 films, nor between the films converted with basic and neutral solutions similarly to what was previously reported in the initial study by Holopainen et al [13]. Cross-section thickness analyses of the coatings revealed that even though the calcium carbonate thin film thickness increases linearly based on the number of ALD process cycles, this behaviour changes in the conversion in phosphate solution to hydroxyapatite. After conversion the thin film thicknesses were approximately 300 nm (2000 cycles) and 380 nm (4000 cycles) indicating that some densification is happening in the thicker coating layer compared to the thinner film during the conversion process (Fig. 2).

3.1 Adhesion testing

The results for the adhesion tests are presented in Fig. 3, and based on these results it can be seen that adhesion values are higher with alkaline conversion solution and 4000 ALD cycles compared to adhesion with neutral conversion solution ($p = 0.005$ for 2000 cycles DAP, $p = 0.009$ for 4000 cycles DAP). Increasing the cycle amount from 2000 cycles to 4000 cycles seems to also improve the adhesion ($p = 0.001$) when using alkaline conversion solution. Holopainen et al. also reported that post-conversion annealing improves the adhesion of the coating layer [13], but in current results the difference between annealed and non-annealed coatings is only 0.8 MPa in favour of the annealed coating but the difference is not statistically significant ($p = 0.39$).

Analysis of the samples with FE-SEM revealed that the hydroxyapatite crystals were intact in the adhesion test area after testing in the samples with the highest measured tensile strength, i.e. samples produced with 4000 cycles and alkaline conversion solution. This indicates that the failure mode in these samples was cohesive and the results correlate more with the glue adhesion strength (EA 9466) than with the actual coating adhesion to substrate material. Samples prepared for adhesion testing with EA 9497 glue performed inferiorly in testing, but further inspection with light and electron microscopy revealed that the samples were covered with a thin glue layer after testing, leaving the hydroxyapatite layer underneath intact. After heat treatment we couldn't find any microcracks or other damage to the coating layer, which have been indicated in some earlier studies with heat treatment of HA coatings [14, 26].

After adhesion testing the samples were stained with alizarin red and the stained samples were photographed and surface areas for cohesive and adhesive failure modes were calculated from the pictures. For the annealed samples the surface area analysis was done with non-stained samples under light microscope. Adhesive failure relates to a situation where the coating is detached from the titanium surface, and cohesive failure occurs either inside the coating layer or at the interface between the coating and the glue layer. Mixed failure mode can be defined as a combination of adhesive and cohesive failures, and it has been found that in some previous studies that it is a quite typical failure mode for this testing method [36, 37]. In the

1
2
3
4 stained samples the uncoated titanium surface does not stain with alizarin red, the calcium of
5 the remaining HA layer has red or light green appearance and glue layer stains purple in the
6 process (Fig. 4). The structure of the red and light green areas were also inspected with FE-
7 SEM, where light green areas were confirmed to contain intact nanocrystalline HA structure.
8 The adhesion results have been compiled with failure mode in Fig. 5, and it can be concluded
9 from the results that the measured adhesion strength correlates with adhesive failure portion
10 in such a way that when the adhesive failure mode dominates the measured adhesion values
11 are lower. Similarly, with cohesive failure mode dominating the adhesion values are higher,
12 except for the EA9497 glue samples in which the glue layer the detachment had happened
13 inside the glue layer (low adhesion strength). These findings support the conclusion that with
14 adhesive failure mode samples the separation is happening in the coating-substrate interface
15 and with cohesive failure modes the detachment is happening either inside the coating layer
16 or in the glue-coating interface.
17
18
19
20
21
22
23
24
25
26
27
28
29

30 **3.2 Scratch testing**

31
32
33

34 Macroscopic plastic deformation of the coating produced with alkaline conversion solution
35 and 4000 ALD cycles seemed apparent in scratch testing with the lowest testing force used
36 (14 mN), but it appears from the FESEM pictures that the scratching tip is actually pushing
37 the coating material in front of and under the scratching tip rather than revealing the titanium
38 base material (Fig. 6). This suggests that the coating material has modest cohesive strength,
39 but does not give additional information about the adhesion between the HA and the
40 titanium. As the scratching force increases to 67 mN the groove gets markedly deeper and the
41 width of the groove converges with the width of the scratching tip. Same phenomenon can be
42 seen with samples stained with alizarin red, where with smaller stresses red calcium-
43 containing material is still visible in the groove, but as the force increases to 67 mN pure
44 titanium is revealed in the bottom of the groove (Fig. 7c&d). In the samples produced with
45 2000 cycles this HA delamination can be detected already with a loading level of 40 mN (Fig.
46 7a&b), and when observing these samples with FESEM it appears that the scratching grooves
47 are shallower and narrower than in the samples produced with 4000 cycles. Scratching test
48
49
50
51
52
53
54
55
56
57
58
59
60
61
62
63
64
65

results thus appear to be in accordance with adhesion test results, indicating that the thicker coating layer is superior in adhesion to the titanium substrate compared to thinner coating.

4. DISCUSSION

Ensuring proper adhesion to the implantation site and promoting integration with bone cells are key focus areas in improving the long-term survival of the titanium implants in medical use [38]. Modifying the implant surface by using biologically active coating materials [39], such as bioactive glass [40] or hydroxyapatite [14], has proven to be one of the most promising ways to improve the osseointegration of the implant. Bioactive coatings can be also used to protect the substrate surface [10, 11] from physiological environment as well as wearing or damaging of the surface in the assembly phase and in long-term use, thus leading to lower amount of metal ions released into the surrounding tissues [41].

In this paper we have studied the mechanical properties of a nanocrystalline hydroxyapatite coating converted from atomic layer deposited calcium carbonate thin film, resulting in highly conformal and uniform coating layer that can be applied on complex three dimensional structures. Relatively low process temperatures compared to other manufacturing methods help to reduce residual stresses and cracking of the coating layer. With a final coating thickness of less than 400nm the surface features aimed for better cell attraction and adhesion are not covered by the coating layer, which can be an issue with other thicker HA coating methods such as plasma spraying. Thickness of the ALD calcium carbonate thin film can be controlled by adjusting the number of ALD cycles, but after conversion to nanocrystalline HA the final coating thickness does not increase linearly, likely due to densification of the coating layer in the conversion phase.

Using adhesion and scratch testing we defined the best process parameter combination for this coating solution, and highest adhesion values were acquired with coating that was produced by 4000 ALD cycles and converted to hydroxyapatite in alkaline solution. Post-conversion annealing at 700°C for 30 minutes improved the adhesion test results by 0.8 MPa compared

1
2
3
4 to non-annealed samples, but the difference was not statistically significant. Based on these
5 measurements the adhesion of ALD HA coating (highest value 6.71 MPa) seems to be lower
6 than reported values for the most widely used plasma sprayed HA coatings (ranging from 10
7 to 60 MPa in different studies [36, 42]). Measurement results are affected by the gluing
8 process parameters such as the amount of glue used, the flatness and cleanliness of the
9 surfaces as well as the surface roughness of the dolly interface, room temperature and relative
10 humidity in the sample preparation area etc. Pretreating the substrate surface before coating
11 with sandblasting, acid-etching or similar methods, could improve the adhesion of the HA
12 coating to the titanium surface significantly [43].
13
14
15
16
17
18
19
20
21

22 However, further examination of the samples under FE-SEM revealed that the hydroxyapatite
23 crystals were intact in the adhesion test area depending on the sample type, and the amount of
24 observed damage correlated with the failure mode. Crystals were undamaged in the samples
25 with dominantly cohesive failure mode, i.e. samples that were produced with 4000 cycles and
26 alkaline conversion solution, and the damage to the hydroxyapatite layer increased with higher
27 adhesive failure percentages. This is in accordance with the previous findings [36, 37] that the
28 adhesion values in pull-out testing represent the bonding strength of both interfaces (between
29 the coating and the substrate and between the coating and the glue) as well as the cohesive
30 strength of the coating and the glue layers. The real adhesion values between the coating and
31 the substrate could thus be higher than what was now measured, which brings into
32 consideration the challenges with current adhesion testing methods [44, 45], and the need to
33 further develop these measurement methods for improving the reliability and comparability
34 of the results [46].
35
36
37
38
39
40
41
42
43
44
45

46 Scratch testing situation compares better to surgical assembly situation and long-term usage
47 wearing conditions, and we find it noteworthy that the coating material seems to first deform
48 under loading and only after increasing the load the coating starts to peel off from the surface.
49 This would indicate that some amount of damage could be tolerated to the coating layer in the
50 assembly phase, which is highly likely to happen in an implant operation.
51
52
53
54
55

56 Considering the implant long-term functionality in physiological environment it could be
57 reasonable to further improve this HA ALD coating method by optimizing the process
58
59
60
61
62
63
64
65

parameters and/or studying the effect of various titanium pre-treatments, such as sandblasting or acid-etching, to the adhesion of the hydroxyapatite coating. Also, further studies are needed to analyze the performance of the HA coating in cell culturing conditions and with human osteoblasts and osteoclasts *in vitro*.

5. CONCLUSIONS

We have shown in this present study that good adhesion can be achieved between the titanium surface and nanocrystalline HA coating produced from ALD manufactured calcium carbonate thin layer. Highest adhesion values were achieved with post-conversion heat treatment in 700 °C for 30 min, with alkaline conversion solution and with higher number of ALD process cycles. Further studies are still suggested to further improve the coating method and to study the adhesion and functionality *in vitro*.

CONFLICT OF INTERESTS

The authors declare that they have no competing interests.

ACKNOWLEDGMENTS

This work was supported by the Finnish Centre of Excellence in Atomic Layer Deposition.

FIGURE CAPTIONS

Fig. 1 a) Top view of nanocrystalline HA on titanium converted from a 4000 cycle film with an alkaline conversion solution and b) the XRD pattern of a HA film on silicon. The peaks of HA (JCPDS no. 09-0432) are represented in the line pattern.

Fig. 2 FESEM cross-sections of HA films on silicon converted from a) 2000 and b) 4000 cycles films with an alkaline conversion solution

Fig. 3 Adhesion test results with standard errors according to sample type. DAP = neutral conversion solution, NH3 = alkaline conversion solution, * indicates $p < 0.01$

Fig. 4 Adhesion test samples stained with alizarin red, failure surface types marked in the picture: pure titanium (white triangle), glue (white arrow), hydroxyapatite (black square). Red and light green HA areas confirmed with FESEM marked to the picture. HA films converted from 4000 cycle films with (a) alkaline conversion solution, (b) neutral conversion solution

Fig. 5 Adhesion strength and proportion of adhesive failure by sample type

Fig. 6: FESEM picture of scratching tip groove, loads a) 14 mN and b) 67 mN, 4000 cycles, alkaline conversion solution

Fig. 7: Scratching test samples stained with alizarin red, alkaline conversion solution, a & b 2000 cycles, c & d 4000 cycles. Base material revealed with a) 40mN and b) 67 mN loading (➤)

6. REFERENCES

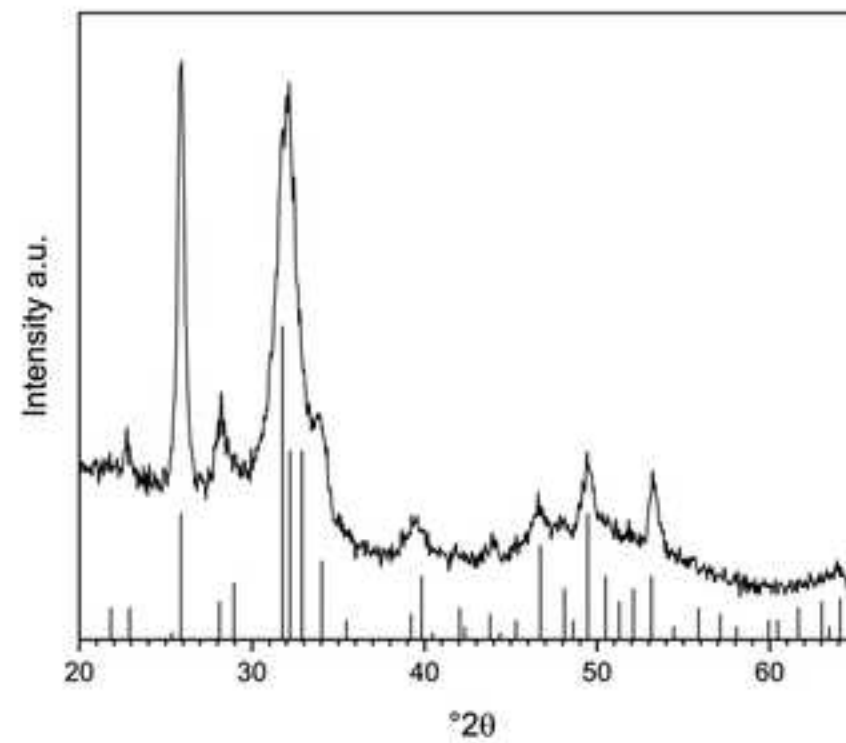
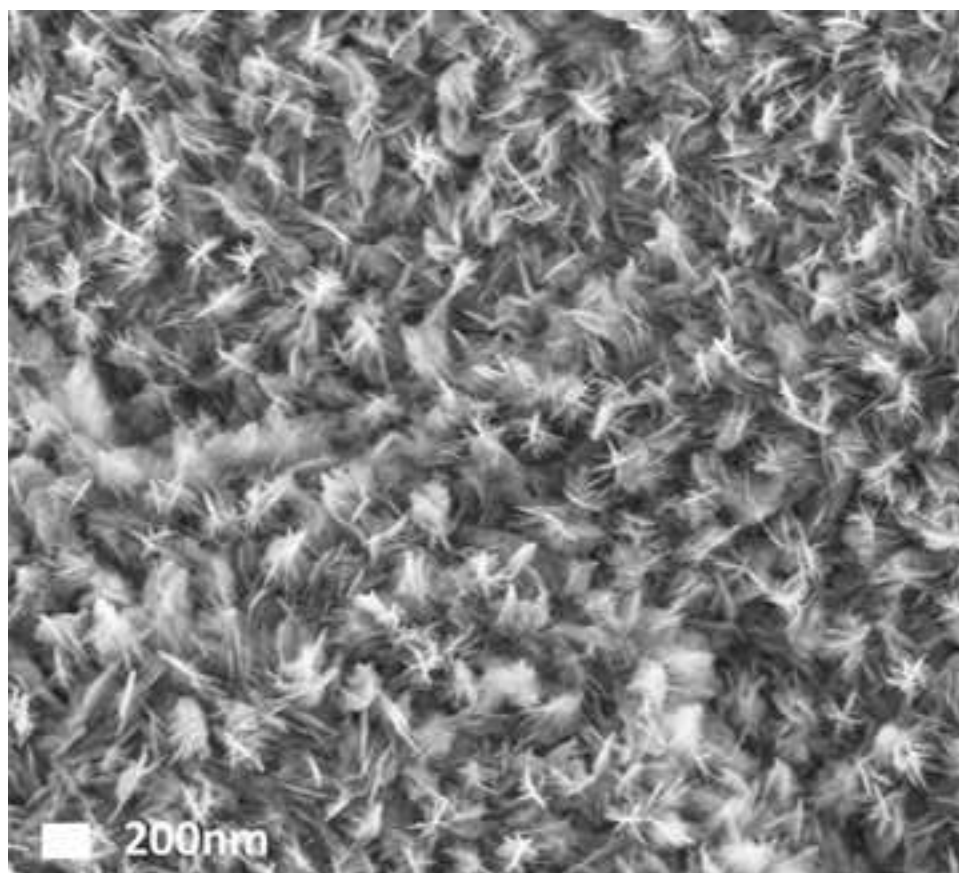
1. Geetha M, Singh AK, Asokamani R, Gogia AK. Ti based biomaterials, the ultimate choice for orthopaedic implants – A review. *Progress in Materials Science* 2009;(54):397-425.
2. Mohseni E, Zalnezhad E, Bushroa AR. Comparative investigation on the adhesion of hydroxyapatite coating on Ti-6Al-4V implant: A review paper. *Int J Adhes Adhes* 2014;(48):238-257.
3. Liu X, Chu PK, Ding C. Surface modification of titanium, titanium alloys, and related materials for biomedical applications. *Mater Sci Eng R Rep* 2004;(47):49-121.
4. Hench LL. The story of Bioglass®. *J Mater Sci Mater Med* 2006;(17):967-978.
5. Sun L, Berndt CC, Gross KA, Kucuk A. Material fundamentals and clinical performance of plasma-sprayed hydroxyapatite coatings: A review. *J Biomed Mater Res* 2001;(58):570-592.
6. LeGeros RZ. Properties of osteoconductive biomaterials: Calcium phosphates. *Clin Orthop Relat Res* 2002:81-98.

7. Coathup MJ, Blunn GW, Flynn N, Williams C, Thomas NP. A comparison of bone remodelling around hydroxyapatite-coated, porous-coated and grit-blasted hip replacements retrieved at post-mortem. *J Bone Jt Surg Ser B* 2001;(83):118-123.
8. Wang H, Eliaz N, Xiang Z, Hsu H-P, Spector M, Hobbs LW. Early bone apposition in vivo on plasma-sprayed and electrochemically deposited hydroxyapatite coatings on titanium alloy. *Biomaterials* 2006;(27):4192-4203.
9. Porter AE, Hobbs LW, Rosen VB, Spector M. The ultrastructure of the plasma-sprayed hydroxyapatite-bone interface predisposing to bone bonding. *Biomaterials* 2002;(23):725-733.
10. Jacobs JJ, Urban RM, Hallab NJ, Skipor AK, Fischer A, Wimmer MA. Metal-on-metal bearing surfaces. *J Am Acad Orthop Surg* 2009;(17):69-76.
11. Mohedano M, Matykina E, Arrabal R, Pardo A, Merino MC. Metal release from ceramic coatings for dental implants. *Dent Mater* 2014;(30):e40.
12. ASTM Standard Specification for Composition of Hydroxylapatite for Surgical Implants. F1185-03 2009.
13. Holopainen J, Kauppinen K, Mizohata K, Santala E, Mikkola E, Heikkilä M, Kokkonen H, Leskelä M, Lehenkari P, Tuukkanen J, Ritala M. Preparation and bioactive properties of nanocrystalline hydroxyapatite thin films obtained by conversion of atomic layer deposited calcium carbonate. *Biointerphases* 2014;(9):031008.
14. Tsui YC, Doyle C, Clyne TW. Plasma sprayed hydroxyapatite coatings on titanium substrates. Part 1: Mechanical properties and residual stress levels. *Biomaterials* 1998;(19):2015-2029.
15. García-Sanz FJ, Mayor MB, Arias JL, Pou J, León B, Pérez-Amor M. Hydroxyapatite coatings: A comparative study between plasma-spray and pulsed laser deposition techniques. *J Mater Sci Mater Med* 1997;(8):861-865.
16. Hsieh M-F, Perng L-H, Chin T-S. Hydroxyapatite coating on Ti6Al4V alloy using a sol-gel derived precursor. *Mater Chem Phys* 2002;(74):245-250.
17. Liu D-M, Yang Q, Troczynski T. Sol-gel hydroxyapatite coatings on stainless steel substrates. *Biomaterials* 2002;(23):691-698.
18. Dinda GP, Shin J, Mazumder J. Pulsed laser deposition of hydroxyapatite thin films on Ti-6Al-4V: Effect of heat treatment on structure and properties. *Acta Biomater* 2009;(5):1821-1830.
19. Nelea V, Morosanu C, Iliescu M, Mihailescu IN. Microstructure and mechanical properties of hydroxyapatite thin films grown by RF magnetron sputtering. *Surf Coat Technol* 2003;(173):315-322.
20. Javidi M, Javadpour S, Bahrololoom ME, Ma J. Electrophoretic deposition of natural hydroxyapatite on medical grade 316L stainless steel. *Mater Sci Eng C* 2008;(28):1509-1515.
21. De Sena LA, De Andrade MC, Rossi AM, De Soares GA. Hydroxyapatite deposition by electrophoresis on titanium sheets with different surface finishing. *J Biomed Mater Res* 2002;(60):1-7.
22. Yang Y, Liu Z, Luo C, Chuang Y. Measurements of residual stress and bond strength of plasma sprayed laminated coatings. *Surf Coat Technol* 1997;(89):97-100.
23. Gross KA, Berndt CC, Herman H. Amorphous phase formation in plasma-sprayed hydroxyapatite coatings. *J Biomed Mater Res* 1998;(39):407-414.

24. Sun L, Berndt CC, Grey CP. Phase, structural and microstructural investigations of plasma sprayed hydroxyapatite coatings. *Materials Science and Engineering: A* 2003;(360):70-84.
25. Zhang Q, Chen J, Feng J, Cao Y, Deng C, Zhang X. Dissolution and mineralization behaviors of HA coatings. *Biomaterials* 2003;(24):4741-4748.
26. Lee EJ, Lee SH, Kim HW, Kong YM, Kim HE. Fluoridated apatite coatings on titanium obtained by electron-beam deposition. *Biomaterials* 2005;(26):3843-3851. DOI:S0142-9612(04)00939-1 [pii]
27. Gross KA, Gross V, Berndt CC. Thermal analysis of amorphous phases in hydroxyapatite coatings. *Journal of the American Ceramic Society* 1998;(81):106-112.
28. Yang Y, Kim K, Ong JL. A review on calcium phosphate coatings produced using a sputtering process—an alternative to plasma spraying. *Biomaterials* 2005;(26):327-337.
29. George SM. Atomic layer deposition: An overview. *Chem Rev* 2010;(110):111-131.
30. Miikkulainen V, Leskelä M, Ritala M, Puurunen RL. Crystallinity of inorganic films grown by atomic layer deposition: Overview and general trends. *Journal of Applied Physics* 2013;(113):021301.
31. Nilsen O, Fjellvåg H, Kjekshus A. Growth of calcium carbonate by the atomic layer chemical vapour deposition technique. *Thin Solid Films* 2004;(450):240-247.
32. Kukli K, Ritala M, Sajavaara T, Hänninen T, Leskelä M. Atomic layer deposition of calcium oxide and calcium hafnium oxide films using calcium cyclopentadienyl precursor. *Thin Solid Films* 2006;(500):322-329.
33. Tillack B, Heinemann B, Knoll D. Atomic layer doping of SiGe - fundamentals and device applications. *Thin Solid Films* 2000;(369):189-194.
34. Hämäläinen J, Holopainen J, Munnik F, Heikkilä M, Ritala M, Leskelä M. Atomic layer deposition of aluminum and titanium phosphates. *J Phys Chem C* 2012;(116):5920-5925.
35. Putkonen M, Sajavaara T, Rahkila P, Xu L, Cheng S, Niinistö L, Whitlow HJ. Atomic layer deposition and characterization of biocompatible hydroxyapatite thin films. *Thin Solid Films* 2009;(517):5819-5824.
36. Yang YC, Chang E. Influence of residual stress on bonding strength and fracture of plasma-sprayed hydroxyapatite coatings on Ti-6Al-4V substrate. *Biomaterials* 2001;(22):1827-1836.
37. Cheng K, Ren C, Weng W, Du P, Shen G, Han G, Zhang S. Bonding strength of fluoridated hydroxyapatite coatings: A comparative study on pull-out and scratch analysis. *Thin Solid Films* 2009;(517):5361-5364.
38. Reyes CD, Petrie TA, Burns KL, Schwartz Z, García AJ. Biomolecular surface coating to enhance orthopaedic tissue healing and integration. *Biomaterials* 2007;(28):3228-3235.
39. Petrie TA, Raynor JE, Reyes CD, Burns KL, Collard DM, García AJ. The effect of integrin-specific bioactive coatings on tissue healing and implant osseointegration. *Biomaterials* 2008;(29):2849-2857.
40. Gomez-Vega JM, Saiz E, Tomsia AP, Marshall GW, Marshall SJ. Bioactive glass coatings with hydroxyapatite and Bioglass® particles on Ti-based implants. 1. Processing. *Biomaterials* 2000;(21):105-111.
41. Thomas P, Weik T, Roeder G, Summer B, Thomsen M. Influence of surface coating on metal ion release: Evaluation in patients with metal allergy. *Orthopedics* 2016;(39):S30.
42. Ding SJ, Ju CP, Chern Lin JH. Morphology and immersion behavior of plasma-sprayed hydroxyapatite/bioactive glass coatings. *J Mater Sci Mater Med* 2000;(11):183-190.

- 1
2
3
4 43. Man HC, Chiu KY, Cheng FT, Wong KH. Adhesion study of pulsed laser deposited
5 hydroxyapatite coating on laser surface nitrided titanium. *Thin Solid Films*
6 2009;(517):5496-5501.
7
8 44. Arrigoni M, Barradas S, Braccini M, Dupeux M, Jeandin M, Boustie M, Bolis C, Berthe
9 L. A comparative study of three adhesion tests (EN 582, similar to ASTM C633, LASAT
10 (LASer Adhesion Test), and bulge and blister test) performed on plasma sprayed copper
11 deposited on aluminium 2017 substrates. *J Adhes Sci Technol* 2006;(20):471-487.
12
13 45. Hadad M, Marot G, Démarécaux P, Chicot D, Lesage J, Rohr L, Siegmans S. Adhesion
14 tests for thermal spray coatings: Correlation of bond strength and interfacial toughness. *Surf*
15 *Eng* 2007;(23):279-283.
16
17 46. Ollendorf H, Schneider D. A comparative study of adhesion test methods for hard
18 coatings. *Surface and Coatings Technology* 1999;(113):86-102.
19
20
21
22
23
24
25
26
27
28
29
30
31
32
33
34
35
36
37
38
39
40
41
42
43
44
45
46
47
48
49
50
51
52
53
54
55
56
57
58
59
60
61
62
63
64
65

Fig. 1



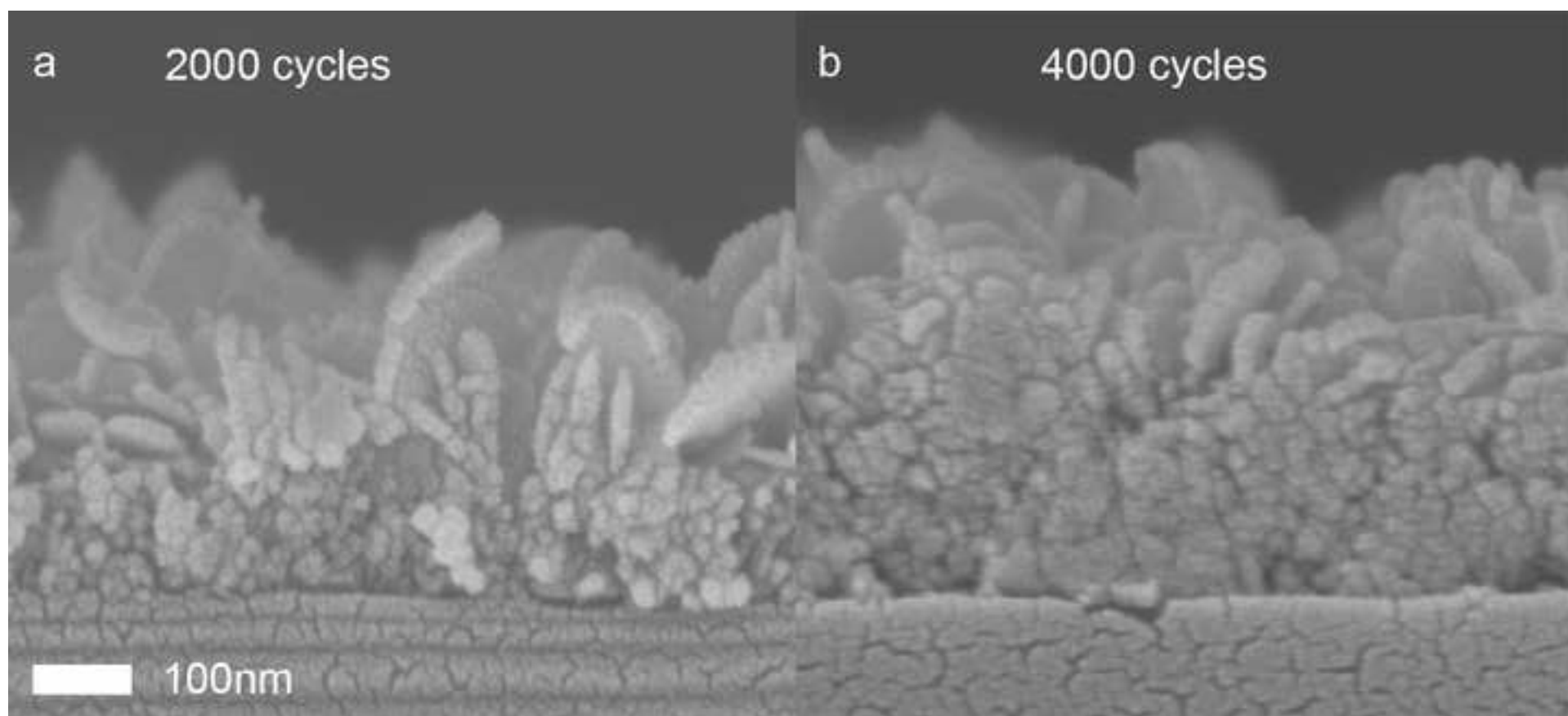


Fig. 3

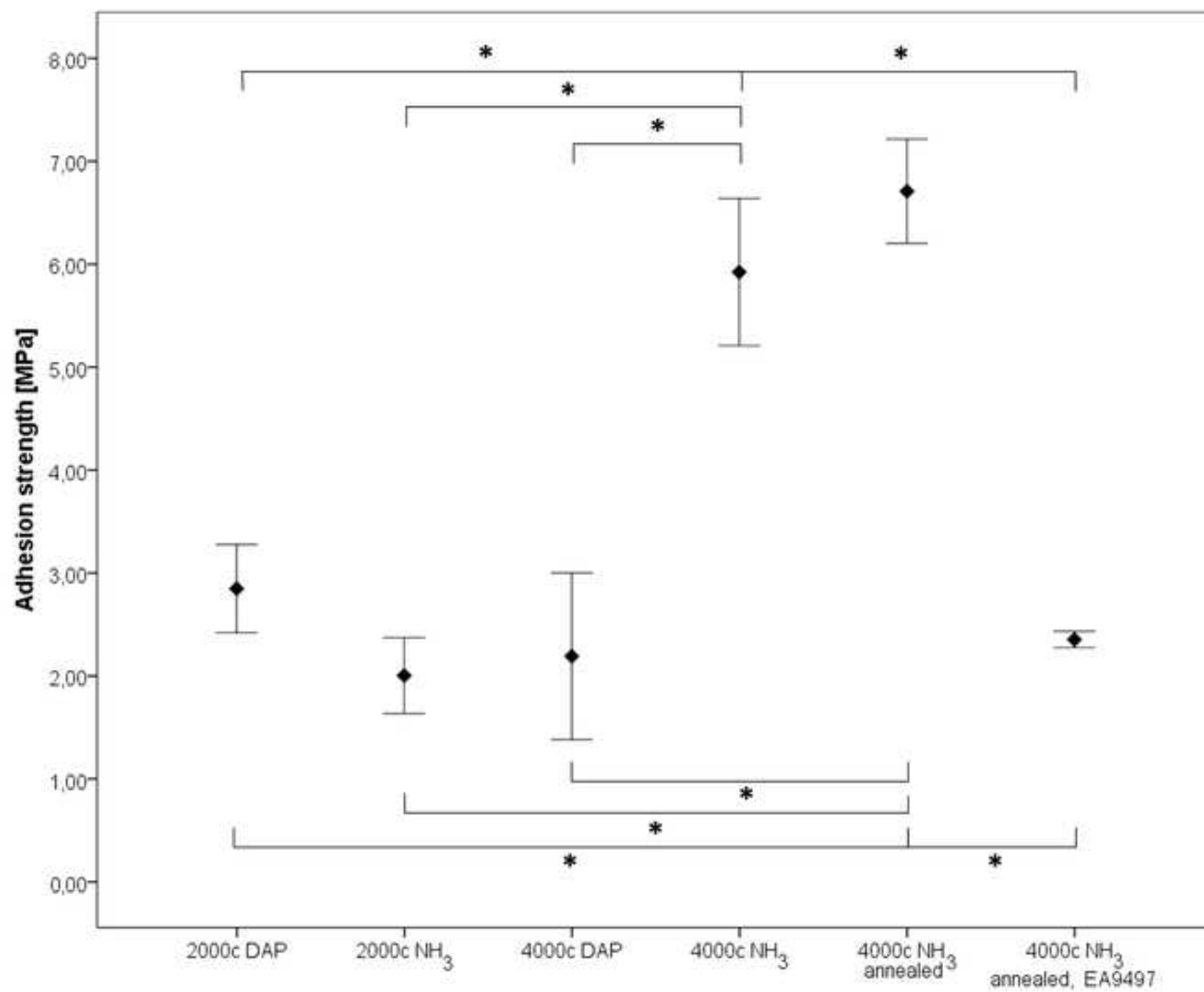


Fig. 4

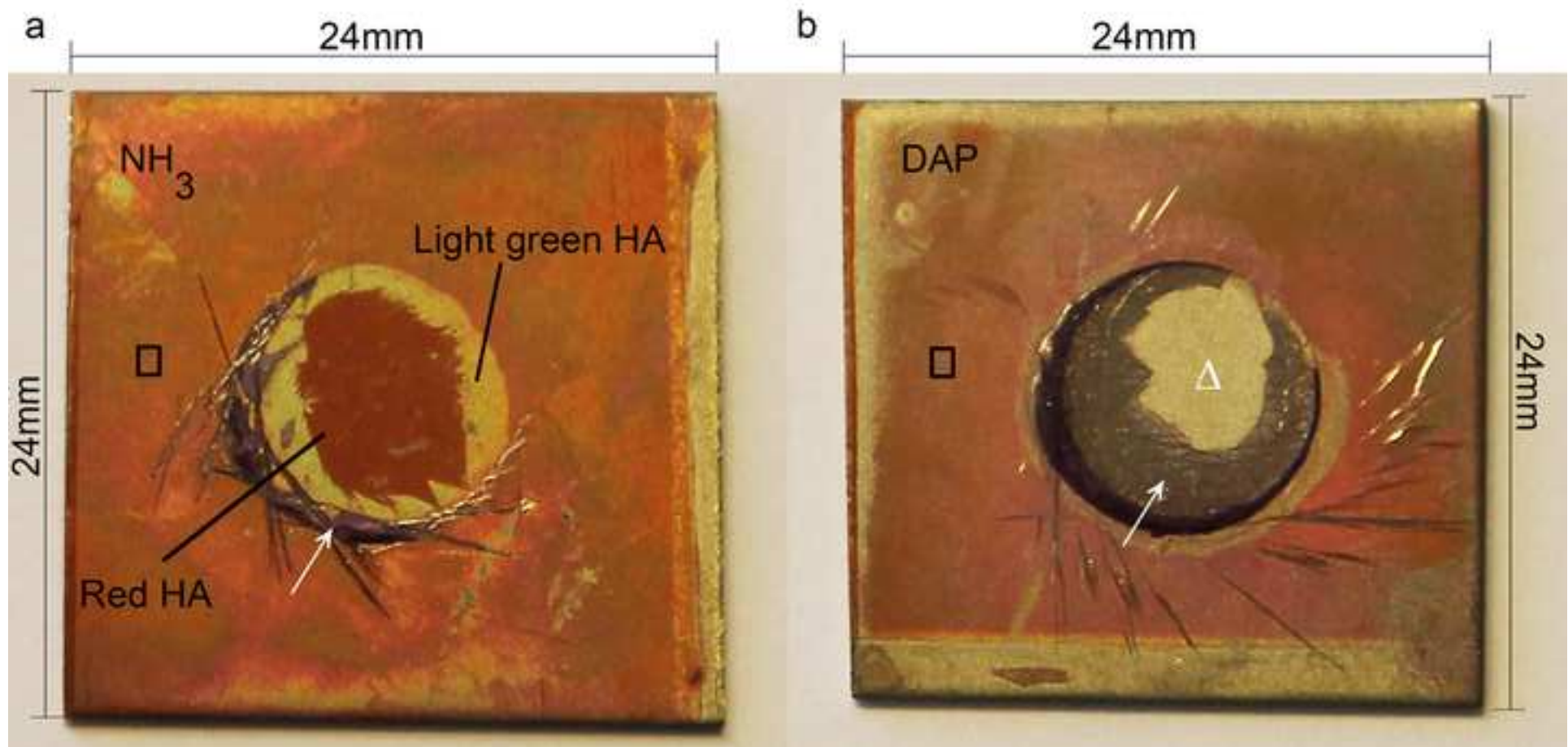
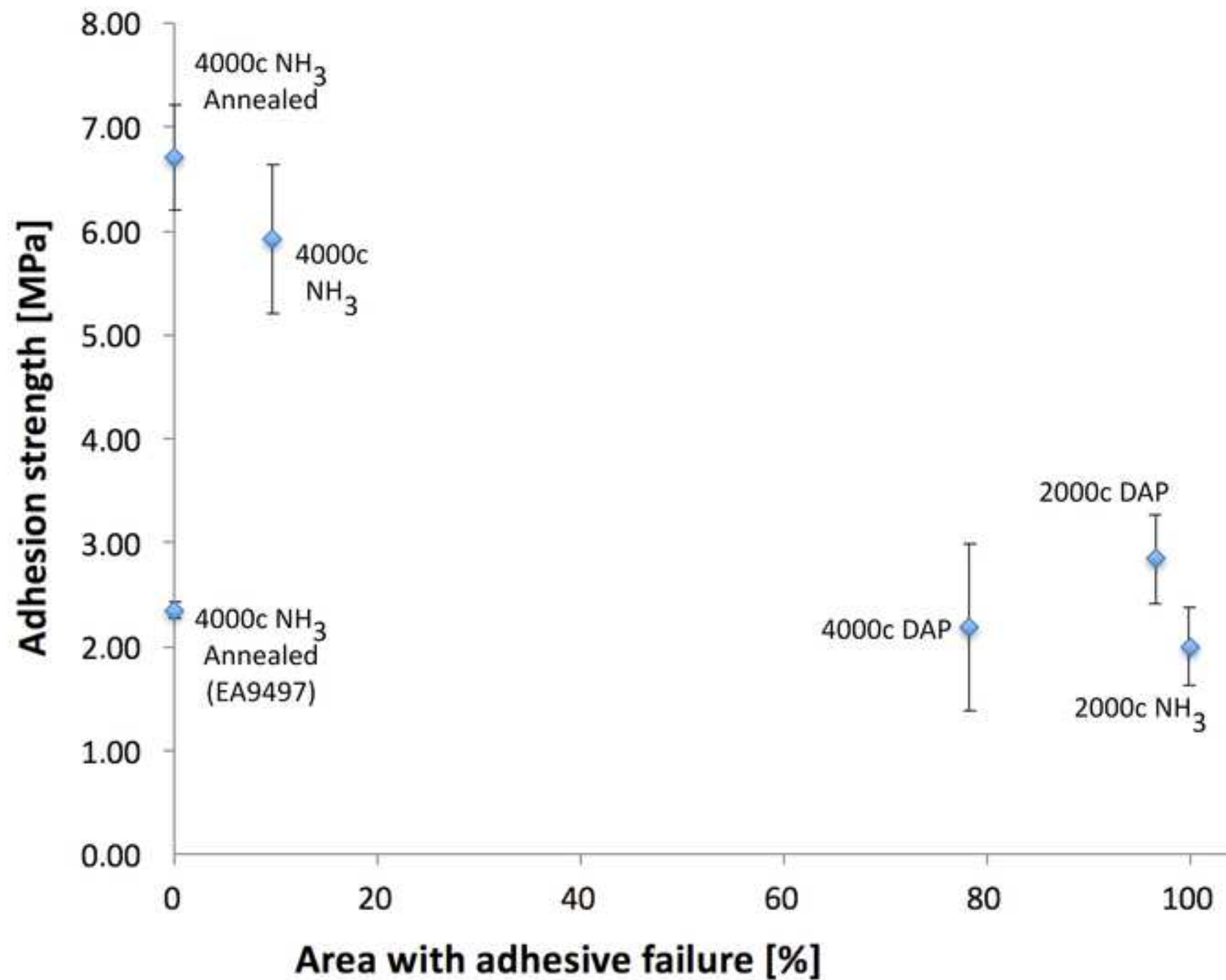
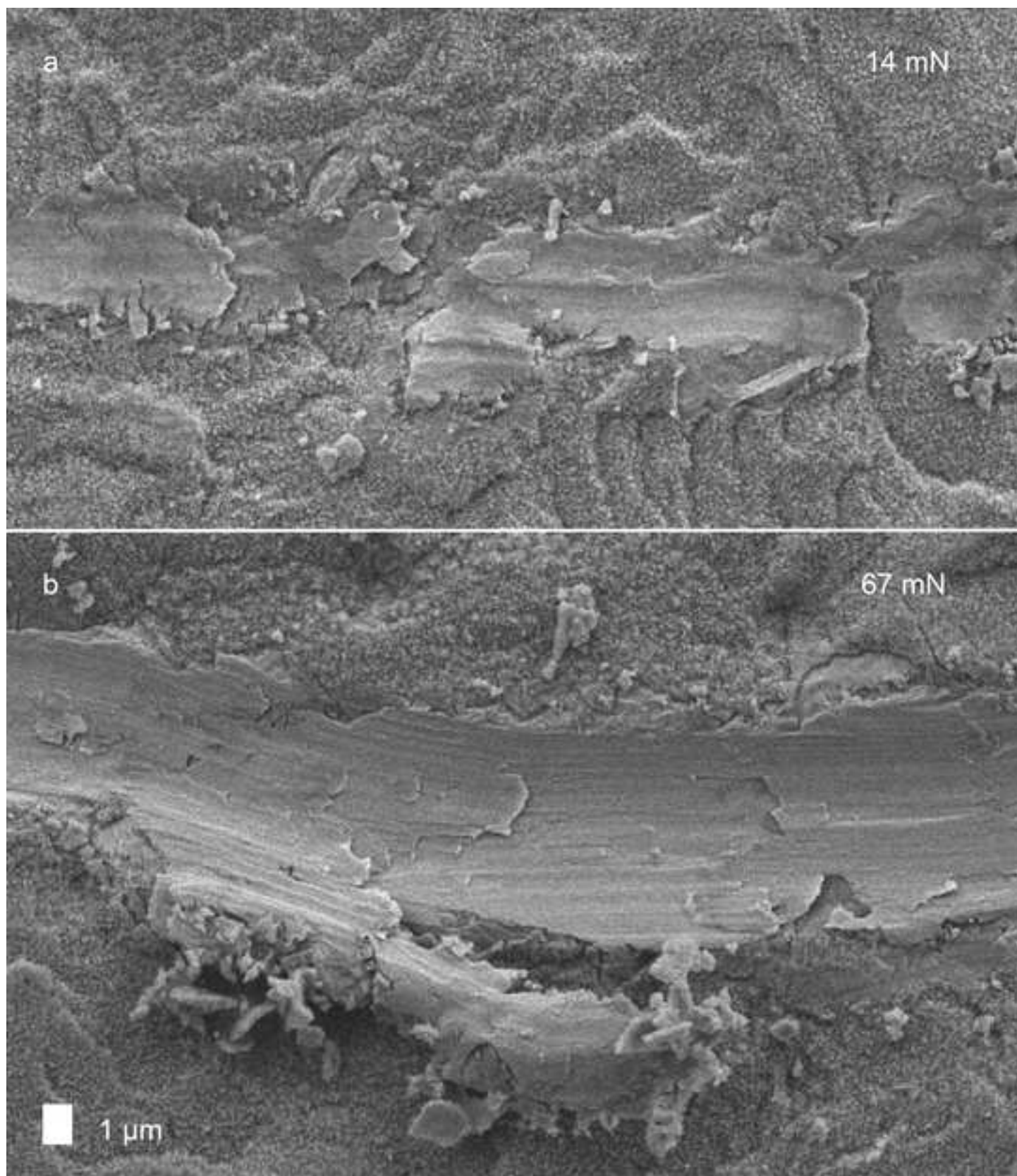
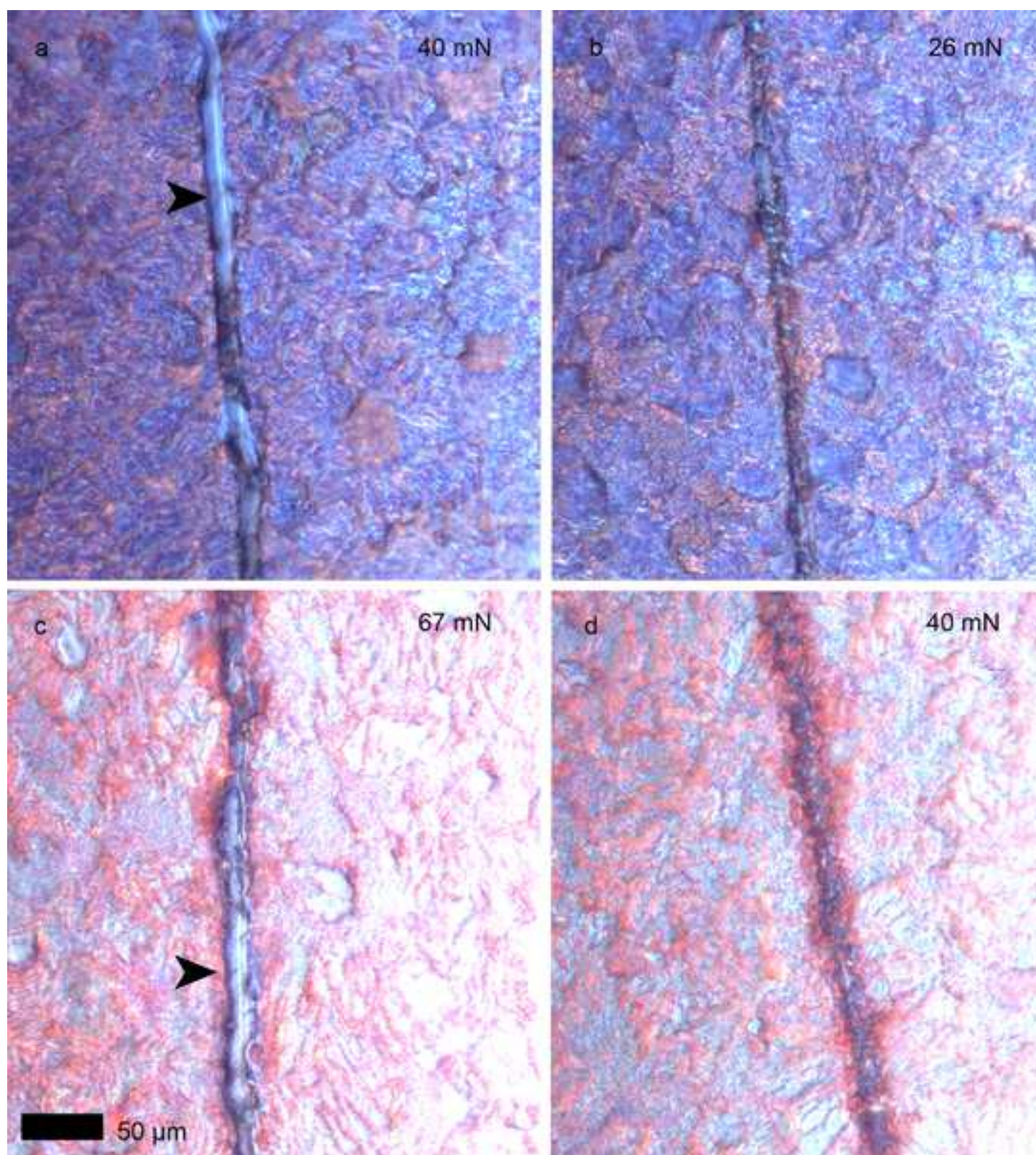


Fig. 5







Titanium implant

